



60 years of fertilization and liming impacts on soil organic carbon stabilization in a sub-tropical Alfisol

Ankita Trivedi¹ · Ranjan Bhattacharyya^{1,2} · Avijit Ghosh³ · Namita Das Saha² · Dipak Ranjan Biswas¹ · Prabhakar Mahapatra⁴ · Shikha Verma⁴ · Dharendra Kumar Shahi⁴ · Shakeel Ahmed Khan² · Arti Bhatia² · Rajesh Agnihorti⁵ · Chamendra Sharma⁶

Received: 2 February 2021 / Accepted: 15 April 2021 / Published online: 21 April 2021
© Springer-Verlag GmbH Germany, part of Springer Nature 2021

Abstract

Limited information is available on the C stabilization mechanism of tropical soils under different management practices including long-term organic manuring, mineral fertilization alone, or in combination with lime. Hence, to understand the effect of continuous application (for 60 years) of organic manure, fertilizer, and lime alone or in combination on an acidic Alfisol, stabilization of soil organic carbon (SOC) was evaluated under maize (*Zea mays* L.) wheat (*Triticum aestivum* L.) cropping. There were eight treatments that included farmyard manure (FYM) and nitrogen (N) applied in terms of FYM, additional dose of phosphorus (P) and potassium (K) applied in terms of inorganic fertilizer (FYM + P'K'), FYM + P'K' with liming (FYM + P'K' + L) and NPK alone. These treatments were laid in a randomized block design with three replications. Results indicated that FYM + P'K' plots had maximum amount of SOC inside large macroaggregates. The value was 33 and 92% greater than only minerally fertilized (NPK) and unfertilized control plots, respectively, whereas microaggregate-associated C was highest in plots with FYM + P'K' and lime (FYM + P'K' + L), which was 48 and 183% more than unfertilized control and NPK plots, respectively. Inside soil microaggregates, plots under FYM + P'K' had highest labile C, while NPK + L plots had highest recalcitrant C. Plots with organic amendments contained higher glomalin in large macroaggregates. Plots treated with FYM + P'K' had maximum intra-aggregate particulate organic matter within microaggregates inside macroaggregates (iPOM_mM), which was 28 and 74% higher than NPK and unfertilized control plots, respectively. Total C stock inside the protected microaggregates within macroaggregates was maximum for FYM + P'K' plots. It had 38, 67, and 171% higher C stock than NPK, FYM, and unfertilized control plots, respectively. Interestingly, despite estimated C input in FYM-treated plots was much higher than NPK plots, FYM-treated plots had less C stabilization within microaggregates and within microaggregates inside macroaggregates. Microaggregates within macroaggregates accounted for ~54% of the recalcitrant C content. Thus, macroaggregates stabilization through occlusion of microaggregates was accountable for sequestration of SOC and only FYM application did not promote that mechanism compared to NPK. Carbon stabilization within macroaggregates under FYM plots was mainly governed by amorphous iron oxide.

Keywords Carbon sequestration · Farmyard manure application on equivalent N basis · Microaggregates inside macroaggregates · Glomalin content

Responsible Editor: Kitae Baek

✉ Ranjan Bhattacharyya
ranjanvpkas@gmail.com

¹ Division of Soil Science and Agricultural Chemistry, ICAR-Indian Agricultural Research Institute, Pusa, New Delhi 110 012, India

² Division of Environment Science, ICAR-Indian Agricultural Research Institute, Pusa, New Delhi 110 012, India

³ Division of Grassland and Silviculture Management, ICAR-Indian Grassland and Fodder Research Institute, Jhansi 284003, India

⁴ Department of Soil Science & Agricultural Chemistry, Birsa Agricultural University, Ranchi, India

⁵ Birbal Sahni Institute of Palaeosciences, 53 University Road, Lucknow, Uttar Pradesh 226007, India

⁶ Environmental Sciences and Biomedical Metrology Division, CSIR-National Physical Laboratory, New Delhi 110012, India

Introduction

Soil organic matter (SOM) is key to many soil functions and foundation for maintaining soil quality. So to maintain the soil quality, it is important to have a clear understanding about composition, function, and behavior of SOM. The quality and quantity of SOM depend considerably on the conditions under which soils have developed. Under tropical and subtropical climatic conditions, SOM content is relatively low compared to temperate regions. But irrespective of any agroecosystem, storage of sufficient SOM is crucial for physical, chemical, and biological functioning of soils.

Under hot and humid climate, the turnover rate of SOM is very high (Ghosh et al. 2016). Availability of optimum moisture and temperature causes decomposition of easily degradable portion of SOM and releases CO₂, which is a greenhouse gas (GHG) and may cause environmental hazards. So, long-term storage and effective management of SOM are essential for overall soil benefits. In a global perspective, minimizing CO₂ concentration in atmosphere and increasing soil organic carbon (SOC) can be achieved through feasible means, i.e., by appropriate soil management practices. Sequestration of SOC has many advantages, including restoration of degraded soils, enhanced biomass production, purification of surface and ground waters, and reduction of CO₂ enrichment in the atmospheric (Lal 2004, Kumar and Nath 2019). Thus, understanding SOC storage mechanism and its dynamics is essential to adopt suitable management practices.

Researchers have tried to keep no stone unturned in understanding SOM dynamics. But complexity of SOM composition, varying turnover rates under different climatic conditions, and heterogeneous mineralogical composition of soils along with differential soil biota distribution make it difficult to generalize SOM dynamics globally (Davidson and Janssens 2006, Davidson et al. 2012, Wankhede et al. 2020). The factors regulating SOC dynamics are climate, soil biota, topography, and chemical compositions of soil and management practices. The major mechanisms for SOC stabilization as given by Lützow et al. (2006, 2008) are as follows: (i) spatial inaccessibility of SOC against decomposer organisms caused by the processes that cause the physical occlusion of SOM, (ii) chemical recalcitrance, and (iii) interaction with mineral surfaces (phyllosilicates and oxides of Fe and Al).

Various studies have shown that continued addition of organic manures could augment soil macroaggregation and lead to increased stable C pools. However, research in the past showed that manure applications in the long run increased the macroaggregate dispersion and caused decreased aggregate stability in a Typic Haploboroll (Whalen and Chang 2002). Further studies revealed that addition of high quantity of organics beyond a certain threshold may lessen the glomalin-related soil protein (GRSP) content, subsequently

decreasing the soil aggregate stability by altering GRSP allocations to macroaggregates in a brown soil of China (Xie et al. 2015). Studies on GRSP distributions with organic manure addition and macroaggregate stabilization are limited. Furthermore, various SOC stabilization mechanisms have been proposed by many researchers, most of which are confined to temperate climate (Six et al. 2002, 2004). In tropical and subtropical climatic conditions, the SOC stabilization as impacted by application of mineral fertilizers and manure vis-à-vis by manure addition in combination with mineral fertilizers (NPK) and lime is not well understood (Ghosh et al. 2018). So, the specific objectives of this study were as follows: to evaluate impacts of long-term (60 years) nutrient management practices on surface soil aggregation and soil C stabilization within aggregates; to determine amorphous Fe oxide, glomalin, and C cycling enzymes in surface soils; and to quantify their relationships with SOC within aggregates and aggregate stability. The hypotheses were as follows: (i) long-term integrated nutrient management (farmyard manure (FYM) application based on equal N fertilization + adjusted doses of P and K) augment C stabilization within aggregates over NPK + lime (L) plots, and (ii) integrated nutrient management would affect glomalin, C cycling enzymes, and intra-aggregate particulate organic matter of soil surface more than NPK + L (farmers' practice).

Materials and methods

Experimental site

A permanent trial was initiated in 1956 at Birsa Agricultural University (BAU), Kanke (Ranchi), Jharkhand, India (23°44' N, 85°32' E, 625 m above the mean sea level). The area is having sub-tropical climate with summer temperature reaches to 42 °C. Winter is mild with 23.1 °C average annual temperature. The average annual rainfall is about 1450 mm. The soil is acidic red clay loam (containing 15.3% silt and 36.4% clay) with low to medium available nutrient content. The dominant clay minerals are kaolinite and illite. Initially, soil had pH 5.5; CEC 10.5 cmol (p+) kg⁻¹ soil, bulk density 1.45 Mg m⁻³, and total N 0.067%.

Experimental design and treatments

Eight treatments with three replications each were laid out in a randomized block design (Table 1). Size of each plot was 4 m × 2.5 m. Each year, recommended dose of N–P₂O₅–K₂O at 110–90–70 kg ha⁻¹ were applied to both crops. Nitrogen (in the form of urea) was applied in three split doses, whereas P (in the form of single superphosphate) and K (in the form of muriate of potash) were applied as basal dose. In organically amended plots, FYM was applied equivalent to 110 kg N

Table 1 Treatment details

Treatments	Denoted as	Source of nutrient			Nutrient dose		
		N	P	K	Lime	FYM (Mg ha ⁻¹)	N:P ₂ O ₅ :K ₂ O (kg ha ⁻¹)
Control	Control	–	–	–	–	–	0:0:0
N	N	Urea	–	–	–	–	110:0:0
FYM	FYM	FYM	–	–	–	22.0	0:0:0
NPK	NPK	Urea	SSP	MOP	–	–	110:90:70
FYM + P _(A-X) + K _(B-Y)	FYM + P'K'	FYM	SSP	MOP	–	22.0	0:21.2:15.8
Lime + NPK	NPK + L	Urea	SSP	MOP	LR	–	110:90:70
Lime + FYM + P _(A-X) + K _(B-Y)	FYM + P'K' + L	FYM	SSP	MOP	LR	22.0	0:21.2:15.8
Lime + N	N + L	Urea	–	–	LR	–	110:0:0

Where the subscripts A and B stand for full dose of P and K, i.e., 90 kg P₂O₅ and 70 kg K₂O ha⁻¹, respectively. X and Y represent the amount of P and K present in full dose of FYM applied on N basis to meet 110 kg N ha⁻¹. LR denotes lime applied after calculating lime requirement

ha⁻¹. Additional dose of P and K was applied in terms of mineral fertilizer after deducting the amount present in FYM. Lime requirement was calculated as per Shoemaker buffer method (Shoemaker et al. 1961) and lime was applied at 3–4 Mg ha⁻¹ once in every 4 years.

Crop management practices and estimation of C input

The field was in continuous maize-wheat rotation since 1956. Other crop management details are given in Trivedi et al. (2020). Total C inputs under different treatments by 54 years of maize and 53 years of wheat were estimated following Kundu et al. (2007). Here, FYM contained ~34% C.

Soil sample collection in the field and processing

After wheat harvest (on 29 April 2016), soil samples in triplicates were collected from all plots using a core sampler from four soil depths (0–15, 15–30, 30–45, and 45–60 cm). Sampling from further depth (>60 cm) was not possible because of hard pan. For all soil layers, soil bulk density values were computed. Treatment and depth wise soil samples in triplicates were bulked to get one bulk sample per plot. After collection, samples were air-dried under shade, followed by grinding and sieving to gently pass through an 8-mm sieve for further analysis.

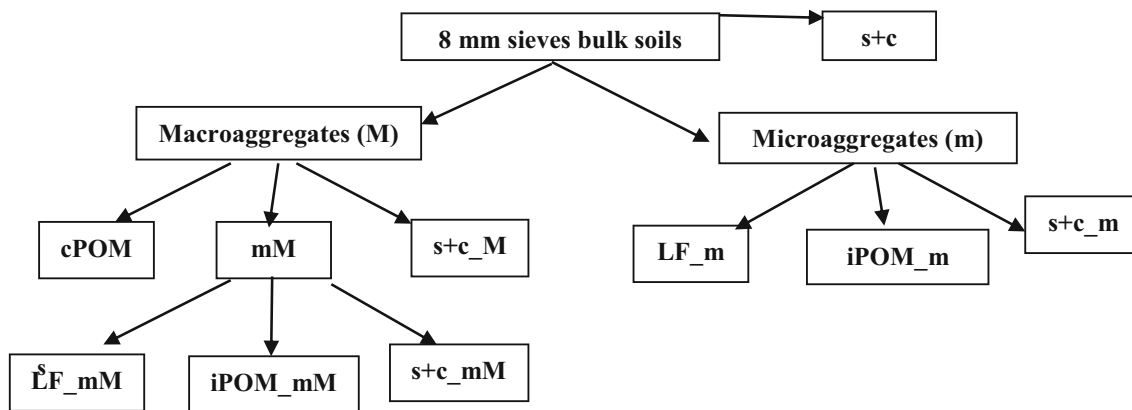
Separation of soil aggregate

By using three sieves, four soil aggregate size fractions were separated by wet sieving of soil samples (< 8 mm) (Elliott 1986). The aggregate fractions were as follows: (i) large macroaggregates (>2 mm), (ii) small macroaggregates (0.250–2

mm), (iii) microaggregates (0.053–0.25 mm), and (iv) silt + clay (< 0.053 mm). Soil samples weighing 100 g after sieving through 8-mm sieve were evenly spread on the 2000- μ m sieve followed by submergence in water at room temperature for 5 min, causing the soil to slake. For water-stable aggregate separation, subsequent sieving was done by moving sieves in an up and down motion for 3 min using Yoder's apparatus. The materials remaining on the sieves were collected on pan placed below the set of sieves and were backwashed into four different Whatman No. 1 filter papers placed over funnels mounted on 500-ml conical flasks. Oven drying of all aggregate fractions were done at 50 °C until a constant weight was obtained. The samples were weighed and were stored at room temperature for further analysis.

Size density fractionation and SOC determination

Microaggregates inside macroaggregates were secluded following Six et al. (1998, 2002) with a little modification. Twenty grams of macroaggregates (M) sub-sample was separated into three fractions: microaggregates inside macroaggregates (mM), coarse particulate organic matter inside macroaggregates (cPOM_M), and silt and clay inside macroaggregates (s+c_M). The method of density fractionation for microaggregates (i.e., mM and microaggregates, m) was modified from Six et al. (1998). After cooling to room temperature, 5 g subsamples of mM and m were weighed and suspended in 35 ml 1.85 Mg m⁻³ sodium iodide in 50-ml graduated centrifuge tube (Modak et al. 2020). Intra-aggregate POM (i.e., iPOM_mM or iPOM_m) and silt and clay (i.e., s+c_mM or s+c_m) fractions were separated following Modak et al. (2020). All fractions were dried at 50 °C and weighed. The entire scheme of density fractionation is presented in Fig. 1.



- s+c - silt + clay
- cPOM - course particulate organic matter
- mM - microaggregate inside macroaggregates
- s+c_M - silt + clay inside macroaggregates
- LF_mM - light fraction inside mM
- iPOM_mM - intraparticulate organic matter inside mM
- s+c_mM - silt + clay inside mM
- LF_m - light fraction inside microaggregates
- iPOM_m - intraparticulate OM inside microaggregates
- s+c_m - silt + clay inside microaggregates

Fig. 1 Fractionation scheme adapted from Six et al. (1998, 2002)

SOC of bulk soils and all aggregate size fractions were determined using an isotopic ratio mass spectrometer (IRMS) (Isoprime; Ölsoprime UK) coupled with an Elemental Analyzer (Owens and Rees 1989). SOC content within mM was measured using treatment-wise soil bulk density and proportion of mM values. Total SOC stocks of different soil fractions were calculated.

Determination of carbon cycling enzymes

Activities of soil enzymes such as α -glucosidase (AG) and β -glucosidase (BG) were studied using MUB (4-methylumbelliferone)-based fluorescence indicators such as 4-MUB- α -D-glucopyranoside and 4-MUB- β -D-glucopyranoside as substrate, respectively (Steinweg et al. 2012). As the soil sample is acidic in nature, 50 mM of sodium acetate buffer was prepared. Stock standard solution of 1 mM was prepared by dissolving 17.6 mg of MUB in 100 ml water. For preparation of standard curve, 2.5, 5, 10, 25, 50, and 100 μ M of MUB was prepared after diluting the stock solution. Soil slurry was prepared taking 2.75-g field moist soil in a conical flask. Standard plates were prepared by pipetting 200 μ L of appropriate standards into correct wells of MUB. Ninety-one milliliters of 50 mM buffer was added. The contents were well mixed with glass rod manually and then placed in a shaker for 30 min at a speed of 120 rpm. Contents were allowed to settle down and supernatants were poured into flat and wide petri dish. Eight hundred microliters of soil soup was pipetted into deep well microplates for enzyme activity

measurement. Two hundred microliters of appropriate 200 μ M substrate was pipetted into correct assay wells. The plates were then sealed and mixed well by horizontal motions on a table top. These plates were incubated at 35 °C for 1.5 h. Two hundred fifty microliters from each well was transferred into corresponding well in a flat and transparent bottomed black 96-well plate. Five microliters of 0.5 N NaOH was added to each sample to stop the reaction. The fluorescence reading was taken at 365-nm wavelength, using a spectrophotometer, with an activation at 310 nm. Standard curve for each soil sample was prepared separately to exclude any background fluorescence present in the soil samples. From the standard curves, calculation for each enzymatic activity for each sample was performed separately.

Determination of total glomalin-related soil protein

Total glomalin content in all aggregate fractions obtained after wet sieving was determined using the method as described by Wright and Upadhyaya (1998). 0.5 g soil sample was taken from all aggregate fractions in glass tube. To it, 10 mL of 50 mM citrate buffer (pH 8.6) was added and autoclaved at 121 °C for 1 h. The supernatant was collected after centrifugation at 5,000 rpm for 5 min. Then again in the leftover aggregate residue, 20 ml of the same citrate buffer was added, autoclaved, and centrifuged until nearly clear supernatant was obtained. This way, all the glomalin content in the soil aggregate fraction was pooled and collected in glass tubes. Then 0.5 mL pooled glomalin was pipetted and to it, 5 mL Bradford's

reagent was added. The developed color was measured at 595-nm wavelength using a spectrophotometer. Spectrophotometer reading was adjusted to zero taking blank as reference solution.

Determination of amorphous Fe oxide

Amorphous Fe oxide was determined following McKeague and Day (1966). For this, 0.2 N ammonium oxalate was prepared by dissolving 14.211 g of it in 500 mL distilled water. pH of the solution was attuned to 3 using 1 N oxalic acid. Soil sample from each aggregate fraction (except silt + clay) of 0.25 g was weighed into 50-mL centrifuge tube. The tubes were wrapped with aluminum foil. To it, 10 mL acid ammonium oxalate was added and shaking was done for 4 h. Then the samples were centrifuged for 10 m at 2000 rpm. After centrifugation, the content in centrifuge was filtered using Whatman No. 42 filter paper. Filtrate was transferred to a 100-ml volumetric flask and the volume was maintained up to the mark using distilled water. From this, 50 mL was taken and digested until it became dry. To it, 10 ml di-acid mixture ($\text{HNO}_3:\text{HClO}_4::9:4$) was added and digested. Di-acid treatment was done until the black color disappeared (organic matter removed). Finally, the digested samples were washed with double-distilled water into a 50-ml volumetric flask. Three blanks were also taken without soil in it. Absorbance reading was taken using an atomic absorption spectrophotometer at 247.2-nm wavelength. Absorbance reading of standard was also taken to plot calibration curve.

Statistical analysis

Data obtained for different soil properties were analyzed using analysis of variance (ANOVA) for a randomized block design as described by Gomez and Gomez (1984). Tukey's honestly significant difference (HSD) test was used as a post hoc mean

separation test ($p < 0.05$) using SAS 9.4 (SAS Institute, Cary, North Carolina, USA). The OPSTAT of Hisar Agricultural University, India, was used to establish correlation among different parameters (Sheoran et al. 1998). Microsoft Office Excel 2013 was used to draw all figures.

Results

Soil aggregate size distribution

Small macroaggregates accounted for >50% total aggregates in the 0–15-cm soil layer (Table 2). Large macroaggregates were highest for FYM-treated plots. The concentration of large macroaggregates under FYM plots was 36 and 56% greater than NPK and unfertilized control plots, respectively. But small macroaggregate distribution was maximum for plots treated with NPK + L. The concentration of small macroaggregates (0.25–2 mm) under NPK + L was 26% more than control plots (Table 2). Microaggregate distribution was maximum for FYM + P'K' fertilized plots. In FYM-treated plots, silt + clay fraction was higher than other treatments and least amount was found in case of mineral fertilized (NPK) plots.

Total organic carbon within soil aggregates

Among all treatments, FYM + P'K'-treated plots contained highest SOC within large macroaggregates (Fig. 2). That value was 92 and 33% greater compared with unfertilized control and NPK plots, respectively (Fig. 2). Among the mineral fertilized plots, large macroaggregates of NPK + L plots had 53% higher SOC concentration than unfertilized control plots. All manure containing plots had higher SOC within large macroaggregates compared with NPK-treated plots. The SOC content inside small macroaggregates was also highest for FYM + P'K' plots in surface soil layer followed by FYM +

Table 2 Sand uncorrected soil aggregate distribution ($\text{g } 100 \text{ g}^{-1}$) of bulk soils in 0–15-cm soil depth as affected by 60 years of fertilization and liming under maize-wheat cropping system in an Alfisol

Treatments*	>2 mm	2–0.250 mm	0.250–0.053 mm	< 0.053 mm
Control	11.5d	51.1 cd	28.3b	9.09ab
N	9.50e	57.8bc	23.9c	8.77b
FYM	18.0a	53.7c	16.5d	11.7a
NPK	13.2c	59.4b	25.2bc	2.24d
FYM + P'K'	14.6c	48.9d	33.0a	3.39d
NPK + L	6.91f	64.2a	18.1d	10.8a
FYM + P'K' + L	16.5ab	53.9c	22.3 cd	7.22bc
N + L	9.06e	54.4c	28.4b	8.11b

*See the "Materials and methods" section for treatment details. Means with similar lowercase letters within a column are not significantly different according to Tukey's HSD test

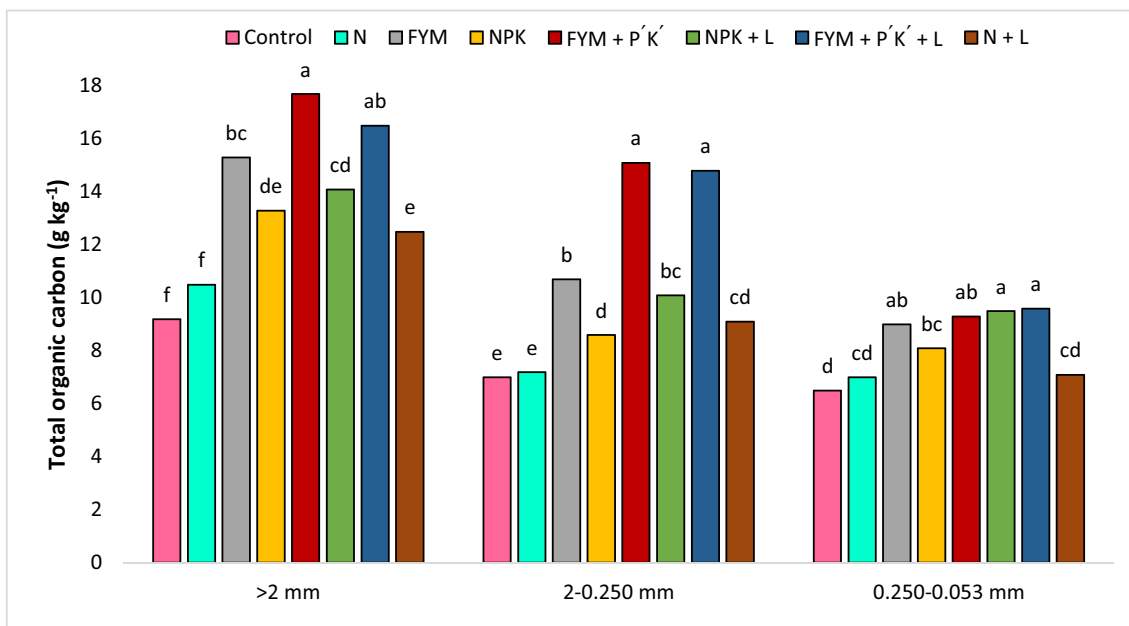


Fig. 2 Total organic carbon concentration (g kg^{-1}) in soil aggregates as affected by 60 years of fertilization and liming under maize-wheat cropping system in an Alfisol. See the “Material and methods” section

for treatment details. Bars with similar lowercase letters within a particular soil size fraction are not significant at $p < 0.05$ according to Tukey’s HSD test

P’K’ + L plots. Highest amount of microaggregate-associated C, which was 48 and 18% higher than control and NPK plots, respectively, was there with FYM + P’K’ + L plots. Plots under FYM, FYM + P’K’ + L and FYM + P’K’ had similar microaggregate-associated C in soil surface (Fig. 2). Likewise, C associated with microaggregates of NPK + L-treated plots was similar to organically amended plots.

Labile and recalcitrant carbon pools of soil aggregates

Large macroaggregates of FYM + P’K’ had 11, 40, and 32% higher labile C compared with FYM, NPK, and unfertilized control plots, respectively (Fig. 3). Similarly, large macroaggregates of FYM + P’K’ plots had highest recalcitrant C, followed by FYM and minerally fertilized plots. Small macroaggregates of FYM + P’K’-treated plots also had highest amount of labile C. Small macroaggregates of FYM + P’K’ plots contained 80, 90, 41, and 12% higher labile C than the small macroaggregates of unfertilized control, NPK, FYM, and FYM + P’K’ + L plots, respectively (Fig. 3).

But unlike labile C, small macroaggregates of FYM + P’K’ + L had 15% more recalcitrant C than FYM + P’K’ plots (Fig. 3). Labile C within microaggregates was similar for unfertilized control and NPK plots and was least for plots treated with N fertilizer alone. Recalcitrant C inside microaggregates was maximum for NPK + L plots, followed by N plots. Interestingly, recalcitrant C within microaggregates of FYM + P’K’ plots was least, despite of having maximum labile C in the same soil fraction.

Distribution of amorphous iron oxide within soil aggregates

Within large macroaggregates, FYM plots contained highest concentration of amorphous iron and the value was 34 and 28% higher compared with NPK and unfertilized control plots, respectively (Table 3). However, amorphous iron oxide concentrations were similar within small macroaggregates of FYM and unfertilized control plots. The least amount of amorphous iron oxide was found in small macroaggregates of FYM + P’K’ + L plots. In general, amorphous iron oxide concentration within small macroaggregates was lesser than large macroaggregates, except for unfertilized control, N, and FYM + P’K’ plots. Within microaggregates of N plots, amorphous iron oxide was highest and that value was 25 and 76% higher than unfertilized control and NPK plots. Least amount of iron oxide was found in the microaggregates of NPK plots.

Total glomalin-related soil protein distribution inside soil aggregates

In all soil fractions, organically amended plots had more GRSP compared with minerally fertilized plots. Plots treated with FYM+P’K’+L had 56 and 18% higher GRSP in large macroaggregates than unfertilized control and minerally fertilized plots (Table 4). Liming also improved distribution of GRSP in large macroaggregates. But it had no influence on GRSP distribution in other aggregate fractions. Glomalin concentrations in small macroaggregates and microaggregates of

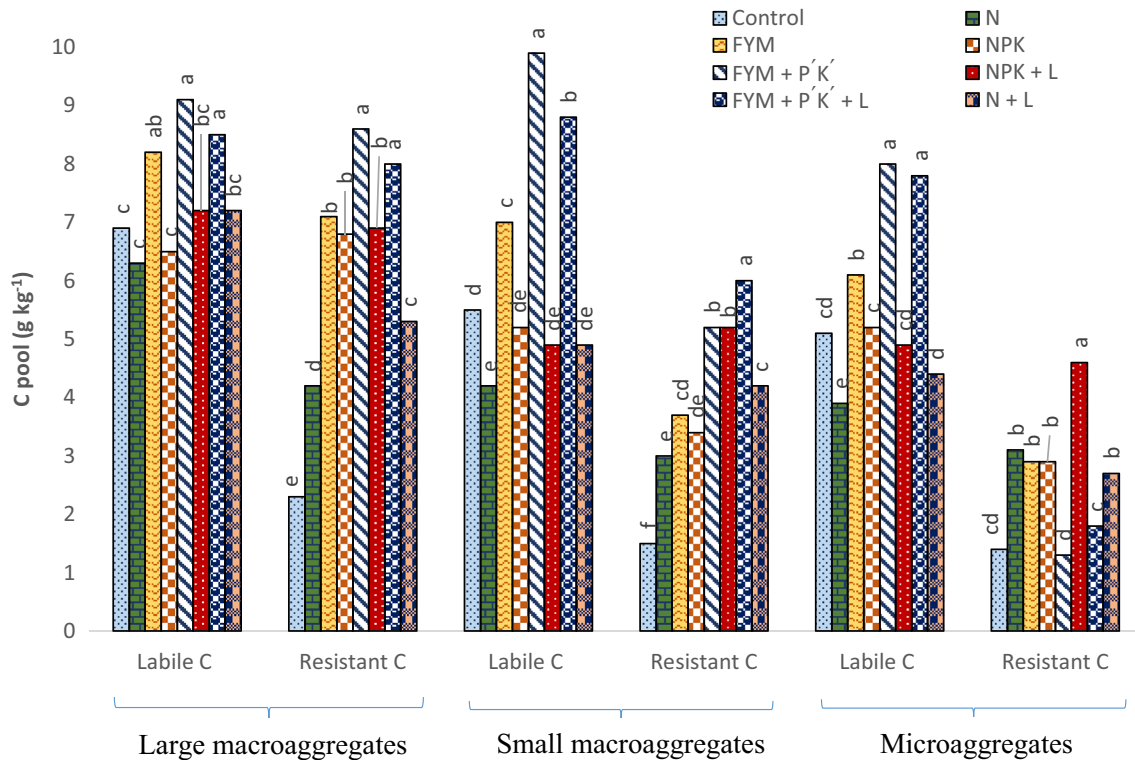


Fig. 3 Labile and resistant soil carbon pools (g kg^{-1}) in soil macroaggregate fractions as affected by 60 years of fertilization and liming under maize-wheat cropping system in an Alfisol. See the

“Material and methods” section for treatment details. Bars with similar lowercase letters within a particular soil size fraction are not significant at $p < 0.05$ according to Tukey’s HSD test

FYM + P’K’ + L plots were highest, followed by FYM + P’K’ plots. Unlike other fractions, highest glomalin concentrations were found within silt + clay fractions under FYM + P’K’ plots. However, GRSP was least in plots treated with only N across the treatments.

Table 3 Amorphous iron oxide concentration in soil aggregates as affected by 60 years of fertilization and liming under maize-wheat cropping system in an Alfisol

Treatments*	Amorphous iron oxide concentration (%)		
	>2 mm	2–0.250 mm	0.250–0.053 mm
Control	0.46bcd	0.56a	0.48bc
N	0.52abc	0.54ab	0.60a
FYM	0.59a	0.56a	0.47bc
NPK	0.44 cd	0.36d	0.34d
FYM + P’K’	0.40d	0.41 cd	0.41 cd
NPK + L	0.53ab	0.45c	0.43c
FYM + P’K’ + L	0.44d	0.36d	0.45bc
N + L	0.48bcd	0.47bc	0.51b

*See the “Materials and methods” section for treatment details. Means with similar lowercase letters within a column are not significantly different according to Tukey’s HSD test

Distribution of microaggregates within macroaggregates (mM), coarse particulate organic matter within macroaggregates (cPOM_M), and silt and clay (s+c_M) within macroaggregates

Plots under N + L plots had 31 and 10% higher cPOM_M than NPK and unfertilized control plots, respectively (Table 5). Among all treatments, NPK + L plots had significantly lower amount of cPOM_M. In general, organically manured plots had lower amount of cPOM_M compared with minerally fertilized plots. However, reverse trend was found for distribution of microaggregates inside macroaggregates (mM). Concentration of mM was more in all plots amended with manure than minerally fertilized plots, except NPK + L-treated plots. Interestingly, microaggregate distribution inside macroaggregates was highest for NPK + L-treated plots. Silt and clay concentration inside the macroaggregates (s+c_M) accounted for <10% value of total macroaggregates. Clay and silt distribution inside macroaggregates did not differ significantly for most of the treatments. Only FYM + P’K’ + L plots had significantly lower s+c_M concentration (< 5%). But the actual amount of cPOM_M in 100 g of bulk soil was found to be highest in FYM+P’K’+L plots and was least in NPK + L plots. Amount of cPOM_M was 12 and 8% higher than NPK and unfertilized control plots, respectively (Table 7). On the

Table 4 Glomalin-related soil protein distribution in soil aggregate fractions as affected by 60 years of fertilization and liming under maize-wheat cropping system in an Alfisol

Treatments*	Glomalin-related soil protein (mg kg ⁻¹)			
	>2 mm	2–0.250 mm	0.250–0.053 mm	< 0.053 mm
Control	1.40b	1.03d	1.00d	0.73bc
N	1.39b	1.06d	0.95d	0.62c
FYM	1.90a	1.60bc	1.54b	0.82b
NPK	1.85a	1.79ab	1.57b	0.71bc
FYM + P’K’	2.00a	1.86ab	1.84a	1.12a
NPK + L	1.85a	1.49c	1.25c	0.69c
FYM + P’K’ + L	2.18a	1.91a	1.90a	1.09a
N + L	1.95a	1.40c	0.95d	0.70c

*See the “Materials and methods” section for treatment details. Means with similar lowercase letters within a column are not significantly different according to Tukey’s HSD test

contrary, amount of mM was highest in NPK + L plots followed by NPK and organically amended plots.

Distribution of soil fractions inside microaggregates within macroaggregates

Light fraction constituted <1% of the microaggregates inside macroaggregates (LF_mM) (Table 6). The highest amount of light fraction was obtained in unfertilized control, followed by FYM + P’K’ plots. But in 100 g bulk soil, concentrations of LF_mM in unfertilized control and FYM + P’K’ plots were similar (Table 7). Plots treated with FYM also had maximum concentration of iPOM inside microaggregates within macroaggregates (iPOM_mM), which was 28 and 74% more than NPK and unfertilized control plots, respectively (Table 6).

Table 5 Percentage distribution (g/100 g of macroaggregate) of sand uncorrected microaggregate (mM), free coarse particulate organic matter between microaggregate (cPOM_M) and silt and clay (s+c_M) within macroaggregate as affected by 60 years of fertilization and liming under maize-wheat cropping system in an Alfisol

Treatments*	(g/100 g of macroaggregates)		
	cPOM_M	mM	s+c_M
Control	60.1b	33.4d	6.57b
N	63.3ab	27.2d	9.57a
FYM	60.3b	31.0 cd	8.75a
NPK	50.2d	43.4b	6.35b
FYM + P’K’	45.5e	45.0b	9.53a
NPK + L	33.7f	56.9a	9.38a
FYM + P’K’ + L	57.9bc	37.9c	4.12c
N + L	65.9a	28.0d	6.03b

*See the “Materials and methods” section for treatment details. Means with similar lowercase letters within a column are not significantly different according to Tukey’s HSD test

Among all plots, manure-treated plots contained higher amount of iPOM_mM than minerally fertilized plots. Least concentration of iPOM_mM was obtained in N + L plots and that value was 18 and 31% less iPOM_mM than unfertilized control and N plots, respectively. But in 100 g of bulk soil, NPK plots had highest amount of iPOM_mM, which was nearly double the amount of unfertilized control plots and the concentration of iPOM_mM was least in N + L plots (Table 7).

Plots under N + L had highest s+c_mM concentration. In general, plots receiving mineral fertilizers had greater s+c_mM concentrations than organically manured plots. The N + L plots had 10 and 16% greater s+c_mM than N- and NPK-treated plots, respectively. But when 100 g bulk soil was considered, NPK + L had highest amount of s+c_mM followed by NPK and organically manured plots (Table 7). Concentration of s+c_mM in NPK + L plots was 42 and 94% higher than that of NPK and unfertilized control plots, respectively.

Distribution of soil fractions within free microaggregates

Amount of light fraction obtained after density fractionation of free microaggregates was very less, that constituted barely 2% of total free microaggregates (Table 6). Among all treatments, plots with N + L treatment had significantly higher amount of light fraction, i.e., 1.7% of total microaggregates. There was not much change in distribution pattern when LF_m concentration in 100 g bulk soil was considered (Table 7). Again N + L plots had highest concentration of the intra-aggregate POM within free microaggregates (iPOM_m). Thus, the plots under N + L had 48, 62, and 38% more iPOM_m compared with N, unfertilized control, and NPK plots, respectively (Table 6). Silt and clay within free microaggregates (s+c_m) was the major constituent of

Table 6 Percentage distribution of light fraction (LF), intra-aggregate POM (iPOM), and silt and clay (s+c) inside microaggregates within macroaggregates (mM) and free microaggregates (m) as affected by 60 years of fertilization and liming under maize-wheat cropping system in an Alfisol

Treatments	(g/100 g of microaggregates within macroaggregate)			(g/100 g of free microaggregates)		
	LF_mM	iPOM_mM	s+c_mM	LF_m	iPOM_m	s+c_m
Control	0.90a	20.8de	78.3ab	0.80c	24.3c	74.9a
N	0.50d	24.8 cd	74.7bc	1.00b	26.7bc	72.3ab
FYM	0.40e	36.2a	63.4e	0.70 cd	30.4b	68.9b
NPK	0.60c	28.3bc	71.1 cd	0.70 cd	28.6b	70.7b
FYM + P'K'	0.70b	27.7bc	71.6 cd	1.00b	36.2a	62.8c
NPK + L	0.50d	20.8de	78.7ab	0.60d	30.7b	68.7b
FYM + P'K' + L	0.40e	29.8b	69.8d	1.00b	30.4b	68.6b
N + L	0.50d	17.1e	82.4a	1.70a	39.4a	58.9c

*See the “Materials and methods” section for treatment details. Means with similar lowercase letters within a column are not significantly different according to Tukey’s HSD test

free microaggregates, accounting for 60–75% (averaged across treatments) of total free microaggregates. In the unfertilized control plots, s+c_m concentration was maximum (74.9%), followed by s+c_m concentrations in N and NPK plots (Table 6). But in 100 g of bulk soil, s+c_m concentration in both unfertilized control and FYM + P'K' plots was similar (Table 7).

Total SOC stock in microaggregates inside macroaggregates and within microaggregates

The C stock in LF_mM was very less compared with all other fractions of soil, despite having higher C concentration owing to its significantly lower weight in bulk soil (Table 9). Total SOC stock in iPOM_mM fraction of FYM+P'K'+L plots was

significantly greater compared with all other treatments (Table 9). The iPOM_mM-associated C stock under FYM + P'K' + L was ~59, 11, and 317% higher than iPOM_mM-associated C stock of FYM, only minerally fertilized (NPK) and unfertilized control plots, respectively (Table 9). The FYM + P'K' and FYM + P'K' + L amended plots had remarkably higher amount of iPOM_mM-associated C stock than the minerally fertilized and unfertilized control plots, except NPK plots.

Averaged across treatments, the s+c_mM fraction had higher total SOC stock than iPOM_mM fraction. Plots under FYM + P'K' had highest s+c_mM fraction-associated C stock, followed by FYM + P'K' + L plots. The s+c_mM fraction-associated C stock in FYM + P'K' plots was ~144 and 51% higher than s+c_mM fraction-associated C of unfertilized control and NPK plots, respectively (Table 9). Total

Table 7 Distribution of all the separated soil fractions (aggregate fractions and size density fractions) within 100-g bulk soil in the 0–15-cm soil depth as affected by 60 years of fertilization and liming under maize-wheat cropping system in an Alfisol

Treatments*	Soil fraction distribution (g/100 g of bulk soil)											
	Soil aggregate fractions			Within macroaggregates (M)			Within microaggregate inside macroaggregate (Mm)			Within free microaggregates (m)		
	M	m	s + c	cPOM_M	mM	s+c_M	LF_mM	iPOM_mM	s+c_mM	LF_m	iPOM_m	s+c_m
Control	62.6c	28.3b	9.09ab	37.6b	20.9de	4.11bc	0.19a	4.35c	16.4e	0.23c	6.88bc	21.2a
N	67.3ab	23.9c	8.77b	42.6a	18.3ef	6.44a	0.09c	4.54c	13.7f	0.24c	6.38bcd	17.3b
FYM	71.7a	16.5d	11.7a	43.2a	22.2d	6.27a	0.09c	8.05ab	14.1f	0.12e	5.02d	11.4d
NPK	72.6a	25.2bc	2.24d	36.4b	31.5b	4.61b	0.19a	8.92a	22.4b	0.18d	7.21b	17.8b
FYM + P'K'	63.5bc	33.0a	3.39d	28.9c	28.6c	6.05a	0.20a	7.92b	20.5c	0.33b	11.9a	20.7a
NPK + L	71.1a	18.1d	10.8a	23.9d	40.5a	6.67a	0.20a	8.42ab	31.8a	0.11e	5.56 cd	12.4d
FYM + P'K' + L	70.4a	22.3 cd	7.22bc	40.8a	26.7c	2.90d	0.11b	7.95ab	18.6d	0.22 cd	6.78bc	15.3c
N + L	63.4bc	28.4b	8.11b	41.8a	17.8f	3.83c	0.09c	3.04d	14.6f	0.48a	11.2a	16.7bc

See the “Materials and methods” section for treatment details. Means with similar lowercase letters within a column are not significantly different according to Tukey’s HSD test

SOC stock of NPK + L plots was similar to FYM + P'K' + L plots. Liming with minerally fertilized plots increased total SOC stock inside s+c_mM fractions (Table 9).

Although SOC stock associated with LF_m and LF_mM was lower in quantity, among all the treatments, total SOC stock was highest in FYM + P'K' plots. Total SOC stock in iPOM_mM fractions was also highest in FYM + P'K' plots. The C stock in iPOM_m fraction of FYM + P'K' plots was 253 and 344% higher compared with control and NPK plots, respectively (Table 9). Plots with NPK + L contained greater iPOM_m fraction-associated C stock than NPK. The s+c_m fraction (inside free microaggregates)-associated SOC stock was less than that of s+c_mM fraction (occluded microaggregates inside macroaggregates)-associated C stock. But s+c_m had higher total SOC stock than iPOM_m fractions. The s+c_m fraction-associated C stock under FYM + P'K' plots was 12, 64, and 72% greater compared with FYM, NPK, and control plots, respectively (Table 9). Total SOC content present inside mM was highest in the FYM + P'K' plots. The FYM + P'K' plots had 69, 35, and 149% higher total SOC content within mM than FYM, NPK, and unfertilized control plots, respectively (Fig. 4). Integration of lime increased mM-associated C content in minerally fertilized plots. Organically amended plots in integration with mineral fertilizers and NPK-treated plots had higher C stock within mM than N + L and unfertilized control plots.

In 60 years, total C inputs under different treatments were estimated from the yield data (Table 8). Results indicate that FYM + P'K' plots had highest and N alone treatment had least C inputs (Table 9). Plots under FYM + P'K' also had highest C stabilization (11 Mg ha⁻¹) within microaggregates inside macroaggregates and within microaggregates (Table 9). Despite higher C input and total SOC concentration within aggregates under FYM-treated plots than NPK plots, C stabilization within microaggregates inside macroaggregates and within microaggregates under FYM only-treated plots was

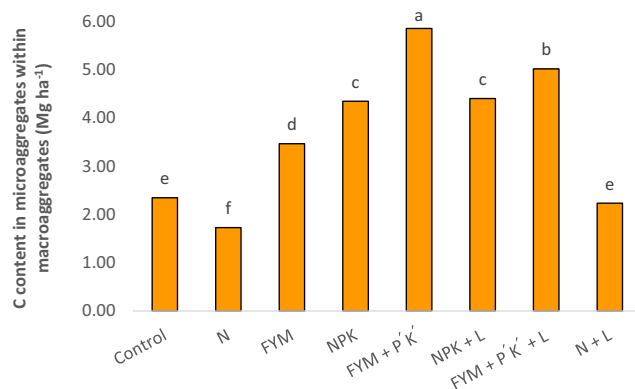


Fig. 4 Total C content of microaggregates within macroaggregates as affected by 60 years of fertilization and liming under maize-wheat cropping system in an Alfisol. See the “Material and methods” section for treatment details. Bars with similar lowercase letters are not significantly different at $p < 0.05$ according to Tukey’s HSD test

~24% less than NPK plots (Table 9). Thus, C stabilization within microaggregates inside macroaggregates and within microaggregates was the major mechanism for NPK and INM plots, whereas amorphous iron oxide binding was the major mechanism for C stabilization within macroaggregates in FYM plots, as FYM-treated plots had highest amorphous iron oxide within aggregates (Table 3). This study also reveals that only FYM application over the years had deleterious effect on C stabilization within aggregates and majority of the C was either lost or present outside aggregates.

Enzyme activity in the bulk soils of surface layer

In FYM + P'K' + L plots, α -glucosidase enzyme was most active among all treatments. Plots under FYM+P'K'+L had 130 and 374% higher α -glucosidase activity than unfertilized control and FYM plots, respectively (Fig. 5). In N and NPK plots, α -glucosidase activity could not be quantified due to development of turbidity in the sample. Least activity of α -glucosidase was obtained in FYM plots. Enzymatic activity of β -glucosidase was also maximum for FYM + P'K' + L plots. Again in this case, detection of zero and low activity of β -glucosidase in N and NPK plots was caused due to development of turbidity in the sample. The MUB-based protocol of enzymatic analysis is extremely sensitive and dependent on the extent of fluorescence emission from each sample. In our experiment, unexplainable turbidity in case of few samples did not allow the fluorescence to emit from them due to the effect of summer sampling, unstable pH of reaction medium, interaction of substrates with soil matrix, etc. Thus, the enzyme activities could not be quantified for those samples.

Correlation among soil aggregation, C associated with aggregates, glomalin content, amorphous Fe content, and C cycling enzymes

In the 0–15 soil layer, percentage distribution of micro- and macroaggregates had negative correlation (Table 10). Microaggregate fractions and amorphous Fe present inside microaggregates were significantly correlated. Both macro- and microaggregate-associated C values had positive correlations with glomalin contents.

Discussion

Long-term effect of liming and fertilization on soil aggregation

More amount of large macroaggregates in FYM-treated plots might be a result of external input of organic matter (Caron et al. 1996). The two main mechanisms responsible for formation of soil macroaggregates due to manuring are (a) free

Table 8 Mean grain yields of maize and wheat of the long-term experiment

Treatments	Mean (of 54 years) maize yield (Mg ha ⁻¹)	Mean (of 53 years) wheat yield (Mg ha ⁻¹)
Control	0.52±0.06e	0.71±0.06d
N	0.44±0.05e	0.17±0.05e
FYM	2.90±0.32b	2.30±0.25b
NPK	1.46±0.14d	1.86±0.19c
FYMP'K'	3.11±0.32b	2.44±0.25b
NPKL	3.97±0.41a	3.61±0.38a
FYMP'K'L	2.91±0.28b	2.18±0.21b
NL	2.36±0.24c	1.67±0.18c

*See the “Materials and methods” section for treatment details. Means with similar lowercase letters within a column are not significantly different according to Tukey’s HSD test

primary particles form microaggregates through bonding with persistent binding agents, afterwards formation of macroaggregates by binding microaggregates through labile binding agents (Tisdall and Oades 1982), and (b) release of bio-products by decomposition of manure and release of gluing substances either by roots or fungal hyphae and/or polysaccharides that cause binding of soil microaggregates subsequently leading to formation of soil macroaggregates (Liao et al. 2006; Sodhi et al. 2009). A good correlation between macroaggregates and total SOC was obtained in this study (Table 10). Increased glomalin-related soil protein (GRSP) in plots amended with organic manure indicates presence of arbuscular mycorrhizal fungi (AMF) in organically manured plots. This is also responsible for increased stability of soil

macroaggregates. The hyphae of AMF bind soil macroaggregates together and provide better soil stability. Contrary to the greater distribution of large macroaggregates in organically manured plots, NPK + L plots had substantially higher amount of small macroaggregates owing to the effect of root biomass in improving soil macroaggregate stability (Pojasok and Kay 1990). Moreover, Ca²⁺ present in lime helps in flocculation of clay particles. Additionally, greater proportions of macroaggregates within plots under FYM and NPK + L than unfertilized control and NPK plots were due to the presence of microaggregates inside it and the binding effect of coarse particulate organic matter (c-POM).

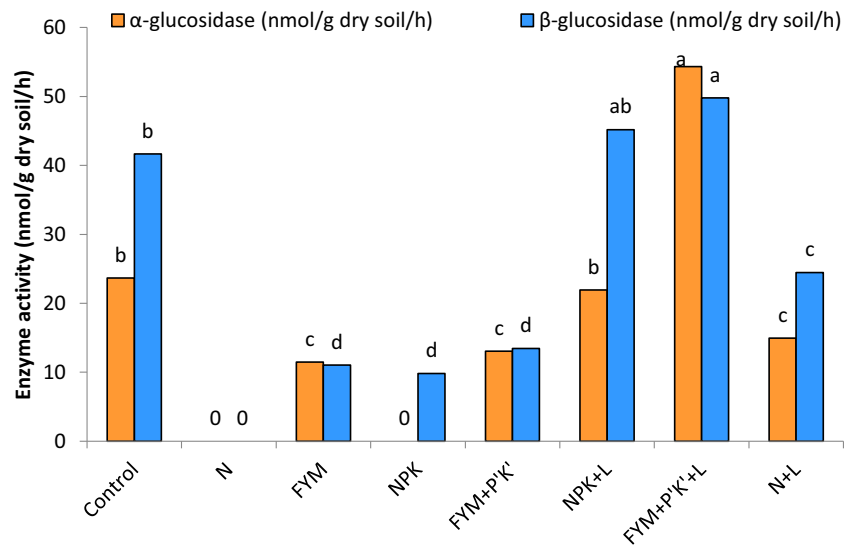
Greater soil aggregation in FYM + P'K' and N + L plots might be due to increased content of glomalin in these plots

Table 9 Total soil organic carbon stock (Mg ha⁻¹) in microaggregates inside macroaggregates and within microaggregates as affected by 60 years of fertilization and liming under maize-wheat cropping system in an Alfisol

Treatments*	Total organic carbon stock (Mg ha ⁻¹)								Estimated carbon input (Mg ha ⁻¹) by 54 years of maize and 53 years of wheat	
	LF_mM	iPOM_mM	s+c_mM	Within microaggregates inside macroaggregates	LF_m	iPOM_m	s+c_m	Within microaggregates		
Control	0.13	0.29de	1.93e	2.35e	0.16	0.34de	2.15c	2.65c	4.99c	24.03 cd
N	0.06	0.15e	1.51f	1.73f	0.17	0.18f	1.75d	2.10d	3.83d	11.20d
FYM	0.08	0.76c	2.63d	3.47d	0.10	0.40 cd	1.68d	2.18d	5.65c	368.34a
NPK	0.13	1.09ab	3.13c	4.35c	0.12	0.27def	2.25c	2.65c	6.99b	64.81c
FYM + P'K'	0.18	0.96bc	4.72a	5.86a	0.29	1.20a	3.70a	5.18a	11.0a	374.92a
NPK + L	0.13	0.41d	3.86b	4.40c	0.07	0.22ef	1.10e	1.39e	5.79c	144.67b
FYM + P'K' + L	0.09	1.21a	3.72b	5.02b	0.19	0.51bc	1.54d	2.24 cd	7.26b	365.68a
N + L	0.04	0.15e	2.04e	2.23e	0.24	0.62b	2.64b	3.51b	5.74c	50.50c

*See the “Materials and methods” section for treatment details. Means with similar lowercase letters within a column are not significantly different according to Tukey’s HSD test

Fig. 5 α -Glucosidase and β -glucosidase activity in bulk soils as affected by 60 years of fertilization and liming under maize-wheat cropping system in an Alfisol. Bars with similar lower-case letters are not significantly different at $p < 0.05$ according to Tukey's HSD test



(Table 3). Furthermore, in those plots, presence of higher amount of iPOM_m helped in binding of microaggregates. In addition, higher silt and clay content of microaggregates could also be the main factor responsible for better aggregation of microaggregates (Amezketta 1999).

Effects of long-term fertilization and liming on total organic carbon within soil aggregates

Greater concentration of total SOC inside macroaggregates than bulk soils might be due to the physical protection exerted by macroaggregates. This could be attributed to (1) decreased oxygen diffusion into macroaggregates (Sexstone et al. 1985; Sollins et al. 1996); (2) the compartmentalization of substrate and microbial biomass (Van Veen and Kuikman 1990; Killham et al. 1993); and (3) the compartmentalization of microbial biomass and microbial grazers (Elliott et al. 1988). Significantly higher amount of total SOC associated with large macroaggregates of FYM-treated plots is caused by enrichment of C due to external input of organic manure (Bhattacharyya et al. 2011). Furthermore, higher amount of total SOC within macroaggregates might be associated with the formation of microaggregates inside macroaggregates. Although microaggregate-associated C concentration is low, it is important for protection of total SOC in soils because of its lower turnover rates.

Long-term fertilization and liming effect on labile and recalcitrant C within soil aggregates

Higher labile C inside large macroaggregates of FYM + P'K' plots is attributed to more C input through FYM. Again, build-up of recalcitrant C in large macroaggregates might be due to poly-condensation of organic matter in plots amended with organic manure for 60 years. From the sequestered organic

carbon quality point, Nardi et al. (2005) found that 40 years of FYM fertilization improved production of humus by 116% with a high degree of polycondensation. But higher recalcitrant C in plots treated with FYM + P'K' + L in small macroaggregates was due to additional effect of liming on better binding and protection of SOM inside small macroaggregates. Least amount of labile C present in microaggregates might be due to better physical protection and decreased microbial access.

Long-term liming and fertilization impacts on amorphous iron oxide distribution within soil aggregates

The study did not show any definite relation between amorphous iron oxide and soil aggregation. This might be due to the variation in crystallinity, particle size, and distribution of the oxides, and to the level at which oxides act. Borggaard (1983) and Bartoli et al. (1991) also showed that the effects of iron oxides on aggregate stability were negligible. However, Goldberg and Glaubig (1987) established that aluminum polymers were more effective in aggregation than iron polymers. However, in this study, higher amount of amorphous iron oxide in large macroaggregates of FYM plots might be due to the binding effect of sesquioxide with organic matter. Higher clay content in microaggregates of N plots might have increased amorphous iron oxide, as sesquioxides can precipitate as gel on clay surface.

Effect of long-term fertilization and liming on total glomalin-related soil protein distribution within soil aggregates

The release of the growth-stimulating substances due to increased soil biological activities and nutrients from organic

Table 10 Pearson's correlations matrix for % macro- and microaggregates, glomalin content, amorphous Fe content, C cycling enzymes, and C associated with aggregates in soil surface

Parameters	% Macroaggregates	% Microaggregates	Glomalin in macroaggregates	Glomalin in microaggregates	Fe in macroaggregates	Fe in microaggregates	α - Glucosidase	β - Glucosidase	Macroaggregates C	Microaggregate C
% Macroaggregates	1.000									
% Microaggregates	-0.798*	1.000								
Glomalin in macroaggregates	0.633NS	-0.234NS	1.000							
Glomalin in microaggregates	-0.177NS	0.614NS	0.545NS	1.000						
Fe in macroaggregates	0.139NS	-0.591NS	-0.473NS	-0.762*	1.000					
Fe in microaggregates	-0.892**	0.772*	-0.651NS	0.123NS	-0.154NS	1.000				
α -Glucosidase	0.028NS	-0.134NS	0.322NS	0.154NS	-0.321NS	-0.146NS	1.000			
β -Glucosidase	-0.030NS	-0.147NS	0.093NS	-0.070NS	-0.252NS	-0.205NS	0.854**	1.000		
Macroaggregate C	0.334NS	-0.111NS	0.854**	-0.653NS	-0.436NS	-0.396NS	0.526NS	0.198NS	1.000	
Microaggregate C	-0.425NS	0.770*	0.330NS	0.941**	-0.790*	0.354NS	0.105NS	-0.040NS	0.506NS	1.000

**Correlation is significant at $p < 0.01$; *correlation is significant at $p < 0.05$; NS non-significant

manure could be the main reason behind higher glomalin in large macroaggregates of organically amended plots. On the contrary, lower glomalin concentration under NPK plots was due to inhibitory effect of mineral fertilizers on development of AMF (Dai et al. 2013). Higher glomalin content in all aggregate fractions under FYM + P'K' + L might be due to suitable soil pH, availability of nutrients, and organic matter. Decreased concentration of glomalin in microaggregates might be due to less labile C availability and absence of oxygen in the well-protected and more stable microaggregates.

Long-term fertilization and liming impacts on distribution of soil fractions present within macroaggregates

Inverse relationship between the distribution of cPOM_M and mM might be due to the fact that cPOM_M are relatively easily decomposable and are greatly depleted upon cultivation (Six et al. 1999). Decomposition of this fraction facilitates gluing of the microaggregates inside macroaggregates, thereby causing better stability of mM fractions of the soils. Increased mM fractions in organically manured plots indicated positive relationship with macroaggregate stability. It means microaggregates inside macroaggregates are responsible for the better stabilization of soil macroaggregates in the organically manured plots. This study could be the first one to our understanding, to report a significant increase in microaggregates inside macroaggregates under a manure-amended surface soil after 60 years of cropping in a subtropical environment.

Long-term effect of fertilization vs liming on aggregation and SOC stabilization

The iPOM_mM fraction is less vulnerable to change in management practices (Six et al. 1998; Modak et al. 2020). Increased concentration of iPOM_mM fractions in plots treated with NPK might be due to increased crop biomass. Inside mM, silt and clay content were remarkably greater indicating higher influence of silt and clay in soil microaggregate stability after 60 years of fertilization. This result is in accordance with Boix-Fayos et al. (2001) who emphasized that microaggregate formation depended on clay content.

However, physical entrapment of the light fraction (LF) material by the heavy fraction and adhesion of the LF to container sides can reduce the efficiency of LF recovery. This might be the cause of lesser amount of m_LF and mM_LF fractions in all treatments. Heavy fractions are often associated with a higher specific density thereby causing greater recovery of iPOM_m and s+c_m fractions. This indicates that iPOM_m and s+c_m fractions are building blocks of microaggregates.

Higher amount of total SOC present in both iPOM_mM and iPOM_m fractions of FYM-treated plots might be due to

the fact that protected POM (iPOM) present inside microaggregates is capable of sequestering the externally applied SOM. But silt and clay fractions contained more total SOC concentration than iPOM fractions of both free microaggregates and microaggregates occluded within macroaggregates. This could be explained by the involvement of persistent binding agent in holding microaggregates and silt and clay particles together. Furthermore, among all treatments, higher amount of total SOC was observed in both iPOM_mM and s+c_mM than iPOM_m and s+c_m fractions, indicating better protection of microaggregates within macroaggregates. Thus, after 60 years of maize-wheat cropping system in an Alfisol, FYM + P'K' plots had 38% more sheltered microaggregate C content compared with NPK in the soil surface.

Long-term fertilization and liming impacts on enzyme activity in the bulk soils of surface layer

Activities of both the C cycling enzymes, i.e., α -glucosidase and β -glucosidase, were maximum in FYM+P'K'+L plots. This might be due to the fact that labile as well as resistant C in this plot was maximum in the surface soil. Microorganisms, being as economic as human being, release their enzyme only for degradation of complex organic matter that constitutes the resistant C. However, FYM and FYM + P'K' plots had more resistant C than minerally fertilized plots, but still showed lower enzyme activity. The reason might be lower pH of FYM and FYM + P'K' (pH=5.31) plots (pH=5.14) than FYM + P'K' + L plots. Likewise, higher enzymatic activity of control plots can be explained by the higher pH value than all other treatments, except FYM + P'K' + L plots. In our experiment, least activity of α -glucosidase was obtained in FYM plots. This least response of α -glucosidase in FYM-treated plots may be because of less available N and P and other mineral nutrients in FYM-amended plots (Liu et al. 2017). Soil sampling during the hot summer (late April 2016) might have decreased soil enzymatic activities. Development of turbidity in the samples of N and NPK plots needs further investigation. Again, pH might be one of the reasons behind development of turbidity as these two plots had lowest pH values (4.48 and 4.69 under N and NPK plots, respectively)

Conclusions

This study is one of the rare attempts to assess soil C stabilization under mineral fertilization (NPK) versus equivalent amounts of NPK when applied under integrated nutrient management (here, FYM + P'K'). Plots treated with FYM + P'K' had 67, 38, and 171% higher C stock in microaggregates inside macroaggregates than FYM, NPK, and unfertilized

control plots, respectively. The microaggregates inside macroaggregates accounted up to 54% of the recalcitrant C content in the soil surface. Thus, stabilization of macroaggregates through occlusion of microaggregates was mainly responsible for sequestration and stabilization of SOM in this agro-ecosystem. The GRSP also played a significant role in stabilization and subsequently increase of resistant C content of macroaggregates under organically manured and NPK + L plots. Amorphous iron oxide played a little role in stabilizing all the fractions of soil aggregates across the treatments. However, amorphous iron oxides played a critical role in C stabilization within macroaggregates in FYM-treated plots (organic agriculture). Higher silt- and clay-associated C concentration inside microaggregates within macroaggregates in FYM + P'K' and FYM + P'K' + L plots indicates their role in stabilization of protected microaggregates. This study highlights the importance of physical as well as biological processes involved in stabilization mechanism of SOM in sub-tropical Alfisol under long-term fertilization and manuring.

Acknowledgements The authors of the ICAR-Indian Agricultural Research Institute thank the Indian Council of Agricultural Research (ICAR) for providing all necessary facilities to carry out this research.

Author contribution Ankita Trivedi and Ranjan Bhattacharyya conceived the idea and Ankita analyzed all the data after collecting soil samples from the experiment that was maintained by Prabhakar Mahapatra, Shikha Verma, and Dharendra Kumar Shahi. Ankita Trivedi, Ranjan Bhattacharyya and Avijit Ghosh developed first draft of the manuscript. Namita Das Saha, Dipak Ranjan Biswas, Shakeel Ahmed Khan and Arti Bhatia reviewed the manuscript and helped Ankita in her analyses. Rajesh Agnihorti and Chamendra Sharma provided the facility to analyze soil organic carbon at the National Physical Laboratory, New Delhi.

Funding This research was funded by the Indian Council of Agricultural Research.

Data availability Materials are not available. The authors have the data.

Declarations

Ethical approval The authors ethically approve the manuscript.

Consent to participate All authors give their consent to participate in this manuscript.

Consent to publish All authors give their consent to publish this manuscript.

Conflict of interest The authors declare no competing interests.

References

- Amezketta E (1999) Soil aggregate stability: a review. *J Sustain Agric* 14: 83–151. https://doi.org/10.1300/J064v14n02_08
- Bartoli F, Philippy R, Doirisse M, Niquet S, Dubuit M (1991) Structure and self-similarity in silty and sandy soils: the fractional approach. *J Soil Sci* 42:167–185. <https://doi.org/10.1111/j.1365-2389.1991.tb00399.x>
- Bhattacharyya R, Kundu S, Srivastva AK, Gupta HS, Prakash V, Bhatt JC (2011) Long term fertilization effects on soil organic carbon pools in a sandy loam soil of the Indian sub-Himalayas. *Plant Soil* 341:109–124. <https://doi.org/10.1007/s11104-010-0627-4>
- Boix-Fayos C, Calvo-Cases A, Imeson AC, Soriano-Soto MD (2001) Influence of soil properties on the aggregation of some Mediterranean soils and the use of aggregate size and stability as land degradation indicators. *Catena* 44:47–67. [https://doi.org/10.1016/S0341-8162\(00\)00176-4](https://doi.org/10.1016/S0341-8162(00)00176-4)
- Borggaard OK (1983) The influence of iron oxides on phosphate adsorption by soil. *Eur J Soil Sci* 34:333–341. <https://doi.org/10.1111/j.1365-2389.1983.tb01039.x>
- Caron J, Espindola CR, Angers DA (1996) Soil structural stability during rapid wetting: influence of land use on some aggregate properties. *Soil Sci Soc Am J* 60:901–908. <https://doi.org/10.2136/sssaj1996.03615995006000030032x>
- Dai J, Hu J, Lin X, Yang A, Wang R, Zhang J, Wong MH (2013) Arbuscular mycorrhizal fungal diversity, external mycelium length, and glomalin-related soil protein content in response to long-term fertilizer management. *J Soils Sediments* 13:1–11. <https://doi.org/10.1007/s11368-012-0576-z>
- Davidson EA, Janssens IA (2006) Temperature sensitivity of soil carbon decomposition and feedbacks to climate change. *Nature* 440:165–173. <https://doi.org/10.1038/nature04514>
- Davidson EA, Samanta S, Caramori SS, Savage K (2012) The Dual Arrhenius and Michaelis-Menten kinetics model for decomposition of soil organic matter at hourly to seasonal time scales. *Glob Chang Biol* 18:371–384. <https://doi.org/10.1111/j.1365-2486.2011.02546.x>
- Elliott ET (1986) Aggregate structure and carbon, nitrogen, and phosphorus in native and cultivated soils. *Soil Sci Soc Am J* 50:627–633. <https://doi.org/10.2136/sssaj1986.03615995005000030017x>
- Elliott ET, Hunt HW, Walter DW (1988) Detrital food-web interactions in North American grassland ecosystems. *Agric Ecosyst Environ* 24:41–56. [https://doi.org/10.1016/0167-8809\(88\)90055-2](https://doi.org/10.1016/0167-8809(88)90055-2)
- Ghosh A, Bhattacharyya R, Dwivedi BS, Meena MC, Agarwal BK, Mahapatra P, Shahi DK, Salwani R, Agnihorti R (2016) Temperature sensitivity of soil organic carbon decomposition as affected by long-term fertilization under a soybean based cropping system in a sub-tropical Alfisol. *Agric Ecosyst Environ* 233:202–213. <https://doi.org/10.1016/j.agee.2016.09.010>
- Ghosh A, Bhattacharyya R, Meena MC, Dwivedi BS, Singh G, Agnihorti R, Sharma C (2018) Long-term fertilization effects on soil organic carbon sequestration in an Inceptisol. *Soil Tillage Res* 177:134–144. <https://doi.org/10.1016/j.still.2017.12.006>
- Goldberg S, Glaubig RA (1987) Effect of saturating cation, pH, and aluminum and iron oxide on the flocculation of kaolinite and montmorillonite. *Clay Clay Miner* 35:220–227. <https://doi.org/10.1346/CCMN.1987.0350308>
- Gomez KA, Gomez AA (1984) *Statistical Procedures for Agricultural Research*, Second Edition, An International Rice Research Institute Book. A Wiley-Inter-Science Publication, Wiley, New York

- Killham K, Amato M, Ladd JN (1993) Effect of substrate location in soil and soil pore-water regime on carbon turnover. *Soil Biol Biochem* 25:57–62. [https://doi.org/10.1016/0038-0717\(93\)90241-3](https://doi.org/10.1016/0038-0717(93)90241-3)
- Kumar N, Nath CP (2019) Impact of zero-till residue management and crop diversification with legumes on soil aggregation and carbon sequestration. *Soil Tillage Res* 189:158–167. <https://doi.org/10.1016/j.still.2019.02.001>
- Kundu S, Bhattacharyya R, Prakash V, Ghosh BN, Gupta HS (2007) Carbon sequestration and relationship between carbon addition and storage under rainfed soybean-wheat rotation in a sandy loam soil of the Indian Himalayas. *Soil Tillage Res* 92:87–95. <https://doi.org/10.1016/j.still.2006.01.009>
- Lal R (2004) Soil carbon sequestration impacts on global climate change and food security. *Science*. 304:1623–1627. <https://doi.org/10.1126/science.1097396>
- Liao JD, Boutton TW, Jastrow JD (2006) Storage and dynamics of carbon and nitrogen in soil physical fractions following woody plant invasion of grassland. *Soil Biol Biochem* 38:3184–3196. <https://doi.org/10.1016/j.soilbio.2006.04.003>
- Liu Z, Rong Q, Zhou W, Liang G (2017) Effects of inorganic and organic amendment on soil chemical properties, enzyme activities, microbial community and soil quality in yellow clayey soil. *PLoS One* 12: e0172767. <https://doi.org/10.1371/journal.pone.0172767>
- Lützw MV, Kögel-Knabner I, Ekschmitt K, Matzner E, Guggenberger G, Marschner B, Flessa H (2006) Stabilization of organic matter in temperate soils: mechanisms and their relevance under different soil conditions - a review. *Eur J Soil Sci* 57:426–445. <https://doi.org/10.1111/j.1365-2389.2006.00809.x>
- Lützw MV, Kögel-Knabner I, Ludwig B, Matzner E, Flessa H, Ekschmitt K, Guggenberger G, Marschner B, Kalbitz K (2008) Stabilization mechanisms of organic matter in four temperate soils: development and application of a conceptual model. *J Plant Nutr Soil Sci* 171:111–124. <https://doi.org/10.1002/jpln.200700047>
- McKeague JA, Day JH (1966) Dithionite-and oxalate-extractable Fe and Al as aids in differentiating various classes of soils. *Can J Soil Sci* 46:13–22. <https://doi.org/10.4141/cjss66-003>
- Modak K, Biswas DR, Ghosh A, Pramanik P, Das TK, Das S, Kumar S, Krishnan P, Bhattacharyya R (2020) Zero tillage and residue retention impact on soil aggregation and carbon stabilization within aggregates in subtropical India. *Soil Tillage Res* 202:104649. <https://doi.org/10.1016/j.still.2020.104649>
- Nardi S, Tosoni M, Pizzeghello D, Provenzano MR, Cilenti A, Sturaro A, Rella R, Vianello A (2005) Chemical characteristics and biological activity of organic substances extracted from soils by root exudates. *Soil Sci Soc Am J* 69:2012–2019. <https://doi.org/10.2136/sssaj2004.0401>
- Owens NJP, Rees AP (1989) Determination of nitrogen-15 at sub-microgram levels of nitrogen using automated continuous-flow isotope ratio mass spectrometry. *Analyst*. 114:1655. <https://doi.org/10.1039/AN9891401655>
- Pojasok T, Kay BD (1990) Effect of root exudates from corn and bromegrass on soil structural stability. *Can J Soil Sci* 70:351–362. <https://doi.org/10.4141/cjss90-036>
- Sexstone AJ, Revsbech NP, Parkin TB, Tiedje JM (1985) Direct measurement of oxygen profiles and denitrification rates in soil aggregates. *Soil Sci Soc Am J* 49:645–651. <https://doi.org/10.2136/sssaj1985.03615995004900030024x>
- Sheoran OP, Tonk DS, Kaushik LS, Hasija RC, Pannu RS (1998) Statistical software package for agricultural research workers. Recent advances in information theory, statistics & computer applications by DS Hooda & RC Hasija Department of Mathematics Statistics, CCS HAU, Hisar, 139-143
- Shoemaker HE, McLean EO, Pratt PF (1961) Buffer methods for determining lime requirement of soils with appreciable amounts of extractable aluminum. *Soil Sci Soc Am J* 25:274–277. <https://doi.org/10.2136/sssaj1961.03615995002500040014x>
- Six J, Elliott ET, Paustian K, Doran JW (1998) Aggregation and soil organic matter accumulation in cultivated and native grassland soils. *Soil Sci Soc Am J* 62:1367–1377. <https://doi.org/10.2136/sssaj1998.03615995006200050032x>
- Six J, Elliott ET, Paustian K (1999) Aggregate and soil organic matter dynamics under conventional and no-tillage systems. *Soil Sci Soc Am J* 63:1350–1358. <https://doi.org/10.2136/sssaj1999.6351350x>
- Six J, Conant RT, Paul EA, Paustian K (2002) Stabilization mechanisms of soil organic matter: implications for C saturation of soils. *Plant Soil* 241:155–176. <https://doi.org/10.1023/A:1016125726789>
- Six J, Bossuyt H, Degryze S, Denef K (2004) A history of research on the link between (micro)aggregates, soil biota, and soil organic matter dynamics. *Soil Tillage Res* 79:7–31. <https://doi.org/10.1016/j.still.2004.03.008>
- Sodhi GPS, Beri V, Benbi DK (2009) Soil aggregation and distribution of carbon and nitrogen in different fractions under long-term application of compost in rice-wheat system. *Soil Tillage Res* 103:412–418. <https://doi.org/10.1016/j.still.2008.12.005>
- Sollins P, Homann P, Caldwell BA (1996) Stabilization and destabilization of soil organic matter: mechanisms and controls. *Geoderma* 74: 65–105. [https://doi.org/10.1016/S0016-7061\(96\)00036-5](https://doi.org/10.1016/S0016-7061(96)00036-5)
- Steinweg JM, Dukes JS, Wallenstein MD (2012) Modeling the effects of temperature and moisture on soil enzyme activity: linking laboratory assays to continuous field data. *Soil Biol Biochem* 55:85–92. <https://doi.org/10.1016/j.soilbio.2012.06.015>
- Tisdall JM, Oades J (1982) Organic matter and water-stable aggregates in soils. *J Soil Sci* 33:141–163. <https://doi.org/10.1111/j.1365-2389.1982.tb01755.x>
- Trivedi A, Bhattacharyya R, Biswas DR, Das S, Das TK, Mahapatra P, Shahi DK, Sharma C (2020) Long-term impacts of integrated nutrient management with equivalent nutrient doses to mineral fertilization on soil organic carbon sequestration in a sub-tropical Alfisol of India. *Carbon Manag* 11:483–497. <https://doi.org/10.1080/17583004.2020.1808766>
- van Veen JA, Kuikman PJ (1990) Soil structural aspects of decomposition of organic matter by micro-organisms. *Biogeochem* 11:213–233
- Wankhede M, Ghosh A, Manna MC, Misra S, Sirothia P, Rahman MM, Bhattacharyya P, Singh M, Bhattacharyya R, Patra AK (2020) Does soil organic carbon quality or quantity govern relative temperature sensitivity in soil aggregates? *Biogeochemistry*. 148:191–206. <https://doi.org/10.1007/s10533-020-00653-y>
- Whalen JK, Chang C (2002) Macroaggregate Characteristics in cultivated soils after 25 annual manure applications. *Soil Sci Soc Am J* 66: 1637–1647. <https://doi.org/10.2136/sssaj2002.1637>
- Wright SF, Upadhyaya A (1998) A survey of soils for aggregate stability and glomalin, a glycoprotein produced by hyphae of arbuscular mycorrhizal fungi. *Plant Soil* 198:97–107. <https://doi.org/10.1023/A:1004347701584>
- Xie H, Li J, Zhang B, Wang L, Wang J, He H, Zhang X (2015) Long-term manure amendments reduced soil aggregate stability via redistribution of the glomalin-related soil protein in macroaggregates. *Sci Rep* 5. <https://doi.org/10.1038/srep14687>